
This is the **accepted version** of the article:

Hu, Kaidi; Torán, Josefina; López-García, Ester; [et al.]. «Fungal bioremediation of diuron-contaminated waters : evaluation of its degradation and the effect of amendable factors on its removal in a trickle-bed reactor under non-sterile conditions». *Science of the Total Environment*, Vol. 743 (November 2020), art. 140628. DOI 10.1016/j.scitotenv.2020.140628

This version is available at <https://ddd.uab.cat/record/238003>

under the terms of the  license

Fungal bioremediation of diuron-contaminated waters: evaluation of its degradation and the effect of amendable factors on its removal in a trickle-bed reactor under non-sterile conditions

Kaidi Hu¹, Josefina Torán¹, Ester López-García², Maria Vittoria Barbieri², Cristina Postigo², Miren López de Alda², Gloria Caminal³, Montserrat Sarrà^{1*}, Paqui Blánquez¹

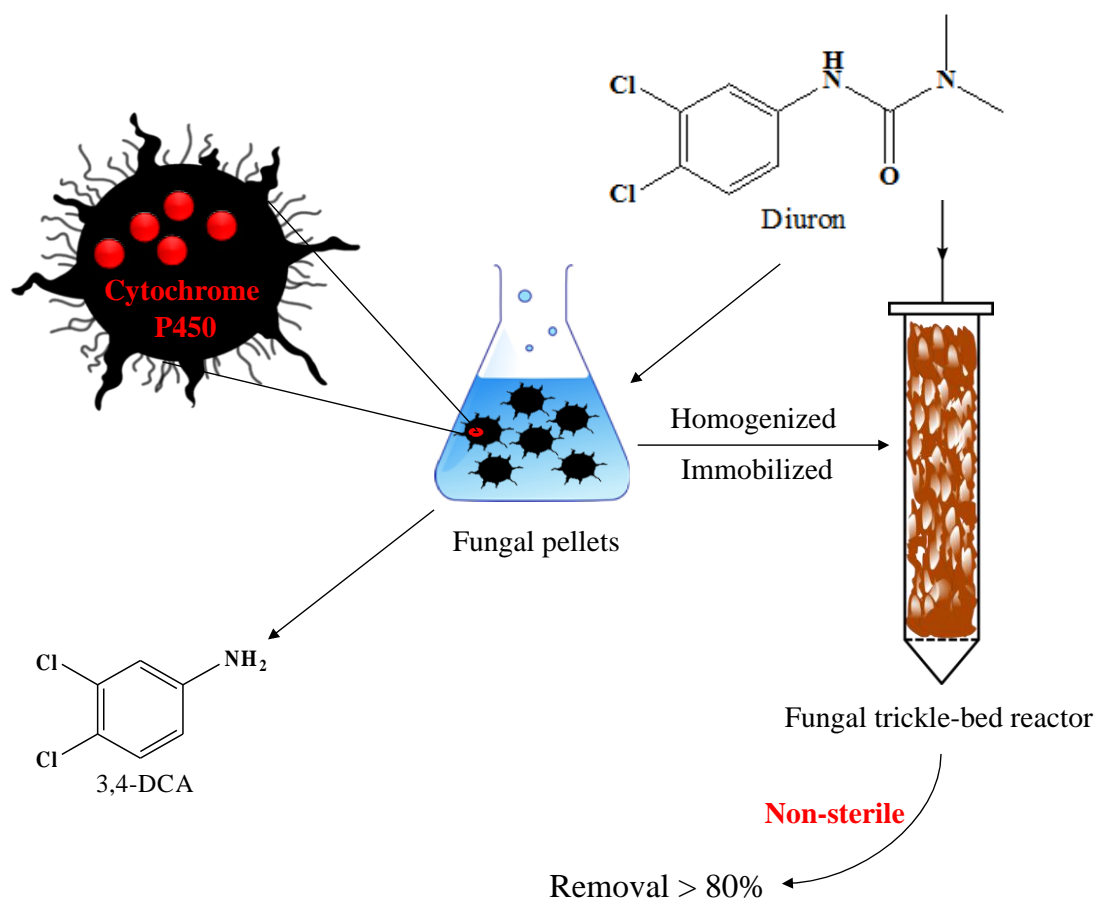
¹Departament d'Enginyeria Química, Biològica i Ambiental, Escola d'Enginyeria, Universitat Autònoma de Barcelona, 08193 Bellaterra, Barcelona, Spain

²Water, Environmental and Food Chemistry Unit (ENFOCHEM), Department of Environmental Chemistry, Institute of Environmental Assessment and Water Research (IDAEA), Spanish Council for Scientific Research (CSIC), Jordi Girona 18-26, 08034 Barcelona, Spain

³Institut de Química Avançada de Catalunya (IQAC), CSIC. Jordi Girona 18-26, 08034 Barcelona, Spain

***Corresponding author:** Departament d'Enginyeria Química, Biològica i Ambiental, Escola d'Enginyeria, Universitat Autònoma de Barcelona, 08193 Bellaterra, Barcelona, Spain. Tel: + 34-34935812789; E-mail: montserrat.sarra@uab.cat

Graphic abstract



Highlights

- *T. versicolor* could effectively degrade both diuron and 3,4-dichloroaniline.
- Cytochrome P450 is involved in diuron degradation by *T. versicolor*.
- Degradation pathway proposed based on metabolites identification.
- Diuron was largely removed in a trickle-bed bioreactor under non-sterile conditions.
- Contact time is a crucial factor according to reactor evaluation.

Abstract

The occurrence of the extensively used herbicide diuron in the environment poses a severe threat to the ecosystem and human health. Four different ligninolytic fungi were studied as biodegradation candidates for the removal of diuron. Among them, *T. versicolor* was the most effective species, degrading rapidly not only diuron (83%) but also the major metabolite 3,4-dichloroaniline (100%), after 7-day incubation. During diuron degradation, five transformation products (TPs) were found to be formed and the structures for three of them are tentatively proposed. According to the identified TPs, a hydroxylated intermediate 3-(3,4-dichlorophenyl)-1-hydroxymethyl-1-methylurea (DCPHMU) was further metabolized into the N-dealkylated compounds 3-(3,4-dichlorophenyl)-1-methylurea (DCPMU) and 3,4-dichlorophenylurea (DCPU). The discovery of DCPHMU suggests a relevant role of hydroxylation for subsequent N-demethylation, helping to better understand the main reaction mechanisms of diuron detoxification. Experiments also evidenced that degradation reactions may occur intracellularly and be catalyzed by the cytochrome P450 system. A response surface method, established by central composite design, assisted in evaluating the effect of operational variables in a trickle-bed bioreactor immobilized with *T. versicolor* on diuron removal. The best performance was obtained at low recycling ratios and influent flow rates. Furthermore, results indicate that the contact time between the contaminant and immobilized fungi plays a crucial role in diuron removal. This study represents a pioneering step forward amid techniques for bioremediation of pesticides-contaminated waters using fungal reactors at a real scale.

1 **Keywords:** White-rot fungi; herbicide removal; transformation products; bioreactor; response
2 surface methodology, high-resolution mass spectrometry

3

4 **1. Introduction**

5 Over the last few decades, pesticide usage has shown a sustained growing tendency as a result of
6 the exponential increase of the human population that brings along the need for intensifying food
7 production. In this context, herbicides act as a key component of modern global agricultural systems
8 (Bilal et al., 2019). Diuron [3-(3,4-dichlorophenyl)-1,1-dimethylurea], a phenylurea herbicide, is
9 used extensively to control weeds throughout the world, not only in agriculture but also in urban
10 and industrial scenarios (Liu, 2014). This herbicide is stable to hydrolysis at neutral pH (pH 5–9)
11 and is generally persistent in soil with a half-life of 320–330 days, and thus, can reach water bodies
12 through leaching or surface runoff (Giacomazzi and Cochet, 2004; Langeron et al., 2014; Liu, 2014).
13 Moreover, its main degradation product, 3,4-dichloroaniline (3,4-DCA) exhibits high toxicity and
14 persistence in soils (Giacomazzi and Cochet, 2004; Tasca and Fletcher, 2018). The presence of
15 diuron in the environment may pose a severe threat to human health and aquatic organisms in several
16 ways (Giacomazzi and Cochet, 2004; Huovinen et al., 2015; Liu, 2014; Mansano et al., 2018). To
17 reduce diuron risks and protect water ecosystems, the European Commission has included this
18 herbicide in the priority hazardous substance list (Directive 2013/39/EU) and established
19 environmental quality standards (EQS) in surface waters. Due to its potential effects, diuron is also
20 one of the 92 substances that are currently being assessed by the European Chemicals Agency
21 (ECHA) as a potential endocrine disruptor. Despite worldwide efforts to control its environmental
22 presence, diuron is still frequently detected in surface and ground waters (Kaonga et al., 2015; Rippy

23 et al., 2017; Santos et al., 2015). Thus, scientific efforts are needed to overcome its persistence and
24 recalcitrance (Liu et al., 2018; López-Ramón et al., 2019; Santos et al., 2019). In this setting, the
25 development of techniques to remove diuron and 3,4-DCA from the environment is strongly
26 motivated and urgent.

27 Bioremediation techniques present two major advantages over both chemical and physical
28 remediation approaches. sustainability and low cost (Azubuike et al., 2016). To date, various
29 microorganisms have been reported to harbor the capacity to simultaneously degrade diuron and
30 3,4-DCA (Ellegaard-Jensen et al., 2013; Sørensen et al., 2008; Sharma et al., 2010; Villaverde et al.,
31 2017). Most of the studies conducted in this line have focused on bacterial species, while white-rot
32 fungi (WRF), that are metabolically versatile and capable of degrading a wide spectrum of
33 xenobiotics due to their nonspecific lignin-degrading enzymes, have only been marginally
34 investigated (Singh and Singh, 2014). Although different reactors based on WRF have been
35 successfully designed for the degradation of various xenobiotics, their implementation at full-scale
36 still needs to overcome some problems, like bacterial contamination (Mir-Tutusaus et al., 2018). In
37 comparison with other reactors such as stirred tank reactor and fluidized bed reactor, trickle-bed
38 reactors (TBR) offer multiple advantages, such as lower operational costs, greater operational
39 flexibility, and higher sustainability (Luo et al., 2014). Furthermore, the immobilization of *T.*
40 *versicolor* on wood has been proven to be advantageous to maintain fungal activity and has been
41 successfully used to remove pharmaceuticals in hospital wastewater (Torán et al., 2017).

42 The purpose of the present study was: i) to screen out one WRF species that could effectively
43 degrade diuron, ii) explore the enzymatic system involved in the degradation, and iii) evaluate the
44 potential transformation products (TPs) formed during the process. A further objective was to

45 estimate the operational variables of a TBR immobilized with the selected fungus for diuron
46 removal, operated under non-sterile conditions, to improve reactor performance and overcome the
47 current limitations for its application in real scenarios.

48

49 **2. Materials and methods**

50 *2.1. Microorganisms and media*

51 *Trametes versicolor* ATCC 42530 was acquired from American Type Culture Collection,
52 *Gymnopilus luteofolius* FBCC 466 and *Stropharia rugosoannulata* FBCC 475 were obtained from
53 Fungal Biotechnology Culture Collection (FBCC) of the University of Helsinki (Finland), and
54 *Pleurotus ostreatus* was isolated from a fruiting body collected from rotting wood (Palli et al., 2014)
55 and preserved in our laboratory. Fungal strains were maintained by subculturing every 30 days on
56 2% (w/v) malt extract plates (pH 4.5) at 25 °C. Blended mycelial suspensions and pellets were
57 prepared using malt extract medium (pH 4.5) as previously described (Blázquez et al., 2004).

58 The defined medium used in the degradation batch experiments in Erlenmeyer regime consisted
59 of (per liter) 8 g glucose, 3.3 g ammonium tartrate, 1.68 g dimethyl succinate, 10 mL micronutrients,
60 and 100 mL macronutrients (Kirk et al., 1978). pH was adjusted to 4.5.

61

62 *2.2. Chemicals and reagents*

63 Diuron (purity, $\geq 98\%$), 3,4-DCA (98%), laccase mediators violuric acid monohydrate (VA, \geq
64 97%) and 2,2'-azino-bis (3-ethylbenzothiazoline-6-sulphonic acid) diammonium salt (ABTS, 98%),
65 cytochrome P450 inhibitor 1-aminobenzotriazole (ABT, purity, 98%), and commercial laccase
66 purified from *T. versicolor* (20 AU mg⁻¹) were purchased from Sigma-Aldrich (Barcelona, Spain).

67 Diuron-d₆, used as a surrogate standard in chemical analyses, was purchased from Toronto Research
68 Chemicals (Ontario, Canada). Hydrated 1-hydroxybenzotriazole (HOBT, ≥ 98%) was obtained from
69 Fluka (Barcelona, Spain). Chromatographic grade acetonitrile was purchased from Carlo Erba
70 Reagents S.A.S (Barcelona, Spain). HPLC-grade methanol, and formic acid (>98%) used as a
71 mobile phase modifier, were obtained from Merck (Darmstadt, Germany). Stock solutions (5 mg
72 mL⁻¹) of diuron and 3,4-DCA to be used in *in vivo* and *in vitro* degradation experiments were
73 prepared by appropriate dilution of the substances in ethanol and stored at – 20 °C until use.

74

75 2.3. Fungal selection for diuron removal

76 To select the best fungal species for diuron removal, degradation experiments were performed
77 in 250 mL Erlenmeyer flasks containing 50 mL of defined medium fortified with diuron at a final
78 concentration of 10 mg L⁻¹. Briefly, pellets of each fungus were transferred into flasks as inoculum,
79 thereby achieving a concentration of approximately 3.4 g dry weight (DW) L⁻¹. Then the cultures
80 were incubated at 25 °C under continuous orbital-shaking (135 rpm) for 7 days. To obviate the
81 influence of photodegradation, the incubation were performed in the dark. Abiotic (uninoculated)
82 and heat-killed culture (121 °C for 30 min) were used as controls. Each set was tested in triplicate.
83 Aliquots were taken at specific time intervals during incubation to measure diuron and glucose
84 concentrations.

85

86 2.4. Evaluation of the enzymatic system involved in diuron degradation

87 *T. versicolor* was selected for subsequent experiments based on its decomposition efficiency. To
88 evaluate the enzymatic system involved in diuron degradation, *in vitro* experiments with *T.*

89 *versicolor* laccase and *in vivo* experiments with an inhibitor of the cytochrome P450 system were
90 conducted.

91 Laccase-mediated degradation experiments were performed in 250 mL Erlenmeyer flasks
92 containing 50 mL laccase-sodium malonate dibasic monohydrate solution (250 mM, pH 4.5) at a
93 final enzyme activity of 500 AU L⁻¹. Diuron concentration was set to 10 mg L⁻¹. Different laccase-
94 mediators including VA, ABTS, and HOBT were added individually to a final concentration of 1
95 mM (Marco-Urrea et al., 2009) for evaluation of their effects on diuron degradation. Abiotic (no
96 laccase) and flasks without the addition of mediators were also prepared as controls. The flasks were
97 incubated for 3 days on an orbital shaker (135 rpm) at 25 °C in the dark and each experimental
98 condition was conducted in triplicate. At selected times, 1 mL sample aliquot was withdrawn from
99 each flask and mixed with 100 µL of 1 M HCl to stop the reaction. Then, it was filtered through a
100 Millipore Millex-GV PVDF 0.22 µm membrane before the analysis of diuron.

101 For evaluating the activity of cytochrome P450, the cytochrome P450 inhibitor ABT (dissolved
102 in ethanol) was added to *in vivo* cultures at 5 mM final concentration (Marco-Urrea et al., 2009).
103 Briefly, experiments in triplicate were carried out in 100 mL Erlenmeyer flasks containing 25 mL
104 of defined medium spiked with diuron at a final concentration of 10 mg L⁻¹. After inoculating
105 pellets (3.2 g DW L⁻¹), cultures were incubated for 7 days at 25 °C in the dark under continuous
106 orbital-shaking (135 rpm). Experimental control was run in parallel in the absence of ABT. Samples
107 were taken at selected times and filtered as mentioned above before the analysis of diuron residues.

108

109 2.5 Identification of diuron transformation products

110 Experiments were conducted in 500 mL Erlenmeyer flasks containing 100 mL of fresh define

111 medium. In brief, after transferring 2.6 g DW L⁻¹ of *T. versicolor* pellets, cultures were incubated
112 for 7 days under the same conditions described in section 2.3. Diuron was added at a concentration
113 of 1 mg L⁻¹. Abiotic control containing only diuron was also prepared. Each experiment was
114 conducted in triplicate. At selected times, 4 mL of the culture was withdrawn and centrifuged (17,
115 700 × g, 4 min) at room temperature. Then, 1.5 mL of supernatant was transferred into a 2-mL amber
116 vial containing 75 µL of diuron-d₆ solution at a concentration of 10 µg mL⁻¹ and kept in the dark at
117 – 20 °C until analysis. Simultaneously, laccase activity was determined during incubation.

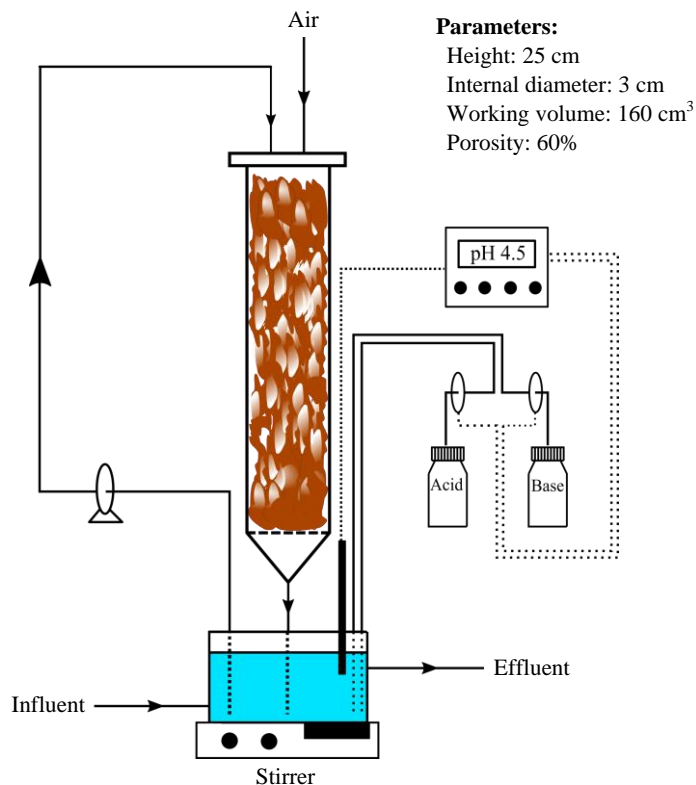
118 Also, another degradation experiment using 3,4-DCA as substrate (10 mg L⁻¹) was performed in
119 parallel, to explore the degradation ability of *T. versicolor* towards the main metabolite formed by
120 diuron and elucidate the biochemical pathway of diuron degradation. In these experiments, 3.2 g
121 DW L⁻¹ of biomass was employed and all the other conditions were identical to those used in diuron
122 degradation experiments (section 2.3). Samples were taken at selected times and filtered as
123 mentioned above before the analysis of 3,4-DCA residues.

124

125 2.6. Diuron removal in fungal TBR under non-sterile condition

126 As shown in Figure 1, a cylindrical glass TBR (Ø 3 cm, h 25 cm) with a working volume of 160
127 cm³ was set up. Specifically, 60 g (29 g DW) of autoclaved wet pine wood chips (2 cm × 1 cm ×
128 0.5 cm) were inoculated with blended mycelial suspension and incubated statically for 9 days as
129 described by Torán et al. (2017). Tap water (adjusted to pH 4.5) was fortified with diuron to a final
130 concentration of 10 mg L⁻¹, and fed into the reservoir bottle from where it was pumped continuously
131 to the top of the reactor through an external recirculation loop. The hydraulic retention time (HRT)
132 corresponding to the total aqueous volume in the system divided by the influent flow rate (F_{in}) was

133 established as 3 days. Humid air was introduced from the top, and the pH was maintained at 4.5 in
134 the reservoir by adding either 1 M HCl or 1 M NaOH, and mixing with a magnetic stirrer.



135
136 **Figure 1** Schematic representation of the trickle-bed reactor set-up
137

138 Response surface methodology (RSM) was applied for assessing the factors that influence diuron
139 removal performance. Given the configuration of this particular system and its variable parameters,
140 recycling ratio (RR), defined as the ratio between recirculating flow rate (F_r) and influent flow rate
141 (F_{in}), and the ratio of influent flow rate to the working volume of the reactor (F_{in}/V_R) were set as
142 independent factors. Correspondingly, the response analyzed was diuron removal at steady state,
143 i.e., after 9 days of continuous treatment. For each experiment, the TBR was newly set up with
144 freshly colonized wood chips. Design Expert V8.06 (Stat-Ease, Inc., MN, USA) was used to design
145 the experiment. A factorial experimental design with 2 factors at 3 levels was employed, as
146 described in Table 1. This translates into 12 experimental runs including 4 replicates.

147

148

149

Table 1 Factors and levels for response surface methodology

Factors	Codes	Levels		
		- 1	0	1
Recycling ratio (RR)	X ₁	200	500	800
F _{in} /V _R (h ⁻¹)	X ₂	0.42	1.04	1.67

150

151 2.7. Analytical methods

152 2.7.1. Biomass quantification

153 Biomass was determined by the dry weight of pellets. It was obtained through filtration of the
154 culture, followed by washing with sterile distilled water and drying at 105 °C to constant weight.

155

156 2.7.2. Glucose concentrations

157 Samples were filtrated through a nylon membrane (0.45 μm) and then measured with a
158 biochemistry analyzer (2700 select, Yellow Springs Instrument, USA).

159

160 2.7.3. Laccase activity

161 Laccase activity was measured through the oxidation of 2,6-dymethoxyphenol (DMP) by the
162 enzyme as described elsewhere (Wariishi et al., 1992). Activity units per liter (AU L⁻¹) are defined
163 as the amount of DMP in μM which is oxidized per minute. The molar extinction coefficient of
164 DMP was 24.8 mM⁻¹ cm⁻¹.

165

166 2.7.4. Diuron and 3,4-DCA concentrations

167 Diuron and 3,4-DCA residual concentrations were determined using high-performance liquid

168 chromatography (HPLC, Ultimate 3000, Dionex, USA) and UV detection. Briefly, 1 mL of culture-
169 aliquot was withdrawn and filtered (0.22 μm , PVDF) before HPLC analysis. HPLC-UV analysis
170 was performed using a C18 reversed-phase column (Phenomenex[®], Kinetex[®] EVO C18 100 Å, 4.6
171 mm \times 150 mm, 5 μm) at 30 °C and a mobile phase consisting of acetonitrile and water (40:60, v/v)
172 at a constant flow rate of 0.9 mL min⁻¹. Analytes were detected using a wavelength of 252 nm. The
173 sample injection volume was 40 μL .

174

175 *2.7.5. Evaluation and identification of TPs*

176 Analysis of TPs was performed using an ultra-high performance liquid chromatography (UHPLC)
177 system Acquity (Waters, Milford, MA, USA) coupled to a hybrid quadrupole-Orbitrap mass
178 spectrometer Q Exactive (Thermo Fisher Scientific, San Jose, CA, USA), equipped with a heated-
179 electrospray ionization source (HESI). Chromatographic separation was achieved with a Purospher[®]
180 STAR RP-18 endcapped Hibar[®] HR (150 \times 2.1 mm, 2 μm) column (Merck, Darmstadt, Germany)
181 and a linear gradient of the organic constituent of the mobile phase. The mobile phase employed
182 under positive ionization mode (HESI+) consisted of (A) water and (B) methanol, both containing
183 0.1% of formic acid (flow rate of 0.2 mL min⁻¹), whereas under negative ionization mode (HESI-)
184 a mobile phase of (A) water and (B) acetonitrile (flow rate of 0.3 mL min⁻¹) was used. The organic
185 gradient applied was: 0–1 min, 5% B; 3 min, 20% B; 6 min, 80% B; 7 min, 100% B; 9 min, 100%
186 B; 9.5 min, 5% B; 14 min, 5% B. The injection volume was 10 μL .

187 The specific conditions used in the HESI interface in both polarity modes were: spray voltage,
188 3.0 kV; sheath gas flow rate, 40 arbitrary units; auxiliary gas, 10 arbitrary units; capillary
189 temperature, 350 °C, and vaporizer temperature, 400 °C. Nitrogen (>99.98%) was employed as

190 sheath, auxiliary and sweep gas. Accurate mass detection was conducted in data-dependent
191 acquisition (DDA) mode. First, a full MS scan was done within the m/z range 70-1,000 at 70,000
192 full width at half maximum (FWHM) resolution(at m/z 200). Then, data-dependent MS/MS scan
193 events (17,500 FWHM resolution at m/z 200) were recorded for the five most intense ions ($>10e^5$)
194 detected in each scan, with a normalized collision energy of 40%. Data acquisition was controlled
195 by Xcalibur 2.2 software (Thermo Fisher Scientific).

196

197 *2.7.6. HRMS data processing*

198 The acquired LC-HRMS data were processed using Compound Discover 3.1 software (Thermo
199 Fisher Scientific). Briefly, experimental samples collected at different times were compared,
200 considering samples collected at $t=0$ as the control. m/z features in the different samples were
201 aligned and deconvoluted using 2 min as maximum retention time shift and 5 ppm of mass tolerance.
202 Then, they were grouped and assigned to a specific molecular ion, for which an elemental
203 composition was predicted. In parallel, a search by formula or mass was performed in various MS
204 libraries and compound databases (ChemSpider, mzCloud, mzVault) for the assignment of a
205 potential compound identity. This workflow produced a list of peaks that was manually revised to
206 identify real TPs, i.e., those peaks that were only present in samples collected after 2 and/or 7 days
207 of degradation, and absent at time 0. Once identified, the molecular structures proposed by the
208 software were evaluated according to the elemental composition of the molecular and fragment ions,
209 fragment rationalization (assisted by fragment ion search scoring), and isotopic patterns.

210

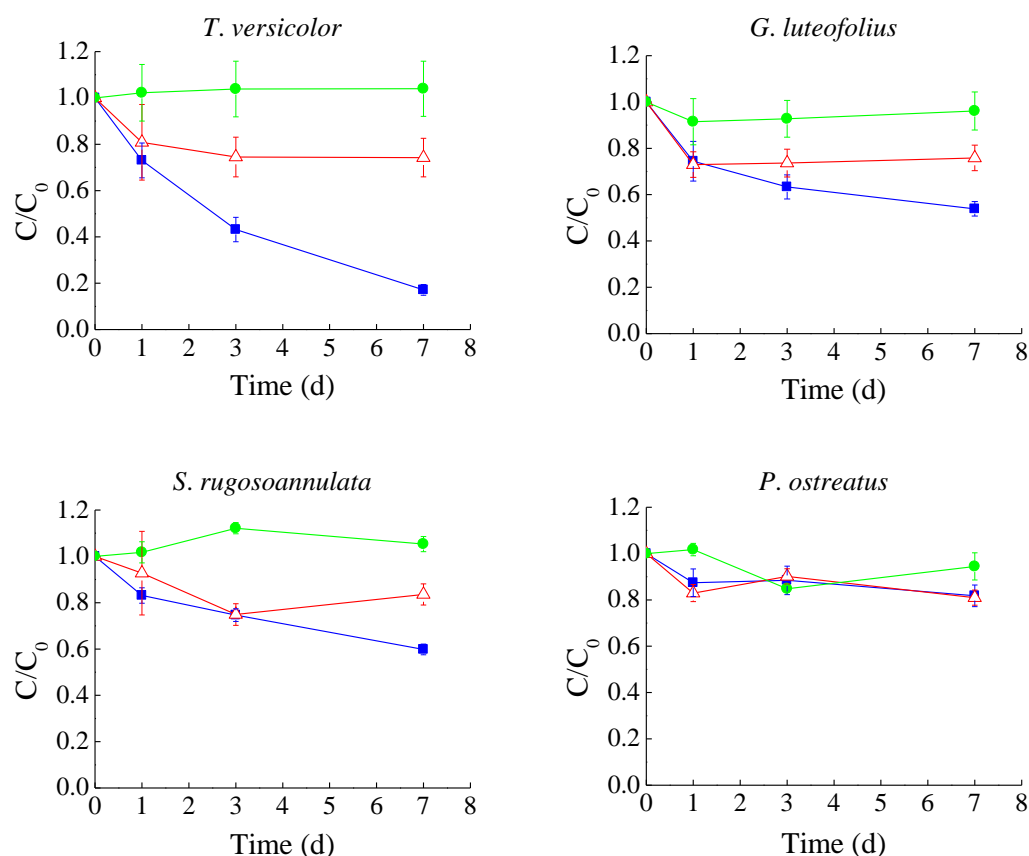
211 *2.7.7. Data analysis*

212 The mean and standard deviation (SD) of data were calculated and subjected to analysis of
213 variance (ANOVA). Statistical significance was determined using SPSS V22.0.

214 **3. Results and discussion**

215 *3.1. Degradation of diuron by different white-rot fungi*

216 Firstly, the ability of different white-rot fungi to degrade diuron was evaluated. As shown in
217 Figure 2, diuron in abiotic controls showed high chemical stability after 7 days of incubation. This
218 means that any removal observed in the experimental treatment must be exclusively attributed to
219 fungal sorption and biodegradation mechanisms. The four tested microorganisms demonstrated
220 different diuron elimination efficiencies, ranging from 18% to 83%. Although there were small
221 differences, the variation patterns of diuron concentration in the different heat-killed fungal cultures
222 were essentially similar, showing an initial fast drop due to sorption onto the biomass, after which
223 concentration remains stable. Thus, sorption contributed to diuron elimination to some extent. This
224 is in agreement with data reported by Lucas et al. (2018) in similar WRF elimination experiments
225 conducted with pharmaceuticals. On average, diuron adsorption observed in this study (16%) was
226 more than double than that observed for other xenobiotics with similar or higher hydrophobicity
227 than diuron (Log Kow 2.68), i.e., venlafaxine (Log Kow 3.28) and carbamazepine (2.45) (Lucas et
228 al., 2018). Thus, additional physical-chemical characteristics may affect the adsorption of the
229 compound onto the biomass (e.g, pKa, or water solubility).



230
 231 **Figure 2** Time-course degradation of diuron by different fungi. C represents the residual
 232 concentration of diuron in the sample (mg L^{-1}), and C_0 corresponds to the initial concentration of
 233 diuron in the sample (mg L^{-1}); Blue lines with filled squares, experimental; red lines with empty
 234 triangles, killed control; green lines with filled circles, abiotic. Average values of three replicates
 235 with the corresponding standard deviation are shown.
 236

237 As for glucose, its concentration plunged to almost zero after 7 days of incubation in *T. versicolor*,
 238 *G. luteofolius*, and *S. rugosoannulata* cultures (Supplementary Information (SI), Table S1).

239 Although the capability of *P. ostreatus* in degrading different xenobiotics such as plastic,
 240 organochlorine pesticides, and polycyclic aromatic hydrocarbons has been well documented
 241 (Bhattacharya et al., 2014; da Luz et al., 2013; Purnomo et al., 2010; Purnomo et al., 2017), an
 242 exceptional scenario was found in diuron degradation, as it presented a much lower consumption of
 243 glucose than the other investigated fungi, with 4.85 g L^{-1} glucose remaining in solution at the end
 244 of the experiment. This is indicative of a lower metabolism of this fungal strain as compared to the
 245 others, which results in nearly no biodegradation (as shown in Figure 2). A similar observation was

246 reported regarding the degradation of venlafaxine by this species in an analogous medium (Llorca
247 et al., 2019), in spite that it showed excellent performance for the removal of other pharmaceuticals,
248 namely, diclofenac, ketoprofen, and atenolol, in sterile hospital wastewater (Palli et al., 2017).
249 Hence, further research is needed to address the mechanisms behind this selective performance.

250 This is the first study that confirms the potential of *S. rugosoannulata* to degrade diuron, thus
251 enriching the diuron-degrading microbe pool. Considering the better performance in diuron
252 degradation by *T. versicolor* compared to the other investigated WRF species, it was selected for
253 further research.

254

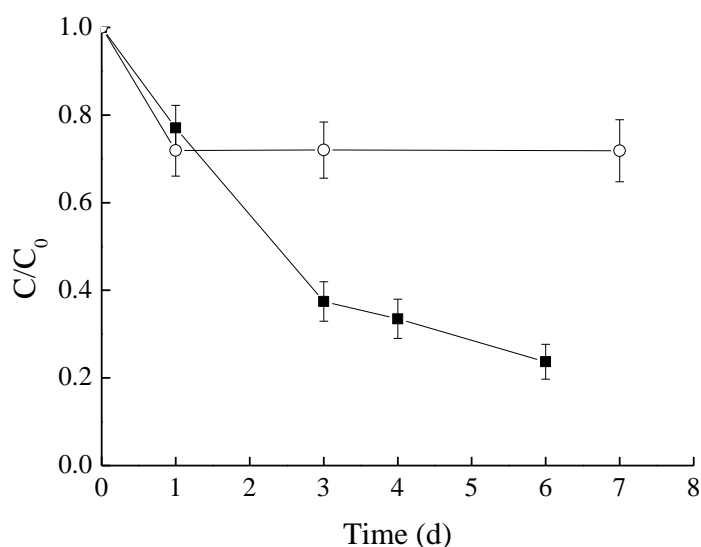
255 3.2. Role of laccase and cytochrome P450 inhibitor in the degradation of diuron

256 Several *in vitro* experiments were carried out to investigate whether laccase and laccase-mediator
257 systems are involved in diuron degradation by *T. versicolor*. Laccase activity was found to reach a
258 maximum level of 27.68 AU L⁻¹ during diuron degradation (TP formation) experiments. Moreover,
259 results of *in vitro* degradation experiments showed that diuron concentrations remained constant
260 throughout the incubation period and were similar to those observed in the abiotic control (Table S2
261 in SI), despite substantial laccase activity (500 AU L⁻¹) was introduced. These results indicate that
262 laccase is not involved in the first step of diuron degradation. Nonetheless, an opposite conclusion
263 was drawn in a previous study (Coelho-Moreira et al., 2018), in which diuron was successfully
264 depleted in the presence of crude laccase from *G. lucidum*, and improved yields were obtained after
265 adding synthetic mediators, namely, ABTS and acetylacetone. Furthermore, Coelho-Moreira et al.
266 (2018) reported that diuron acted as a laccase inducer. The genetic difference among genera and
267 species of WRF could explain the discrepancy of the results obtained. Likewise, the effect of

268 different redox potentials between the laccase enzyme and the monophenolic substrate may be a key
269 factor (Glazunova et al., 2018). In this regard, it is also worthy to point out that low levels of Mn
270 peroxidase were detected in culture filtrate from *G. lucidum* (Coelho-Moreira et al., 2018).

271

272 The activity of the cytochrome P450 enzymatic system in diuron degradation was evaluated *in*
273 *vivo* experiments after the addition of the cytochrome P450 inhibitor 1-aminobenzotriazole. The
274 presence of the cytochrome P450 inhibitor in the culture hindered diuron degradation as compared
275 to the inhibitor-free culture system, although some removal occurred initially, which was probably
276 attributed to sorption processes (Figure 3). This finding is in agreement with previous reports that
277 showed that the addition of 1-aminobenzotriazole significantly inhibited diuron degradation by *P.*
278 *chrysosporium* and *G. lucidum*, as well as the metabolites produced in the process (Coelho-Moreira
279 et al., 2013, 2018).



280

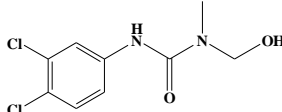
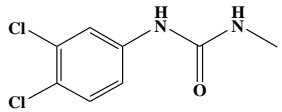
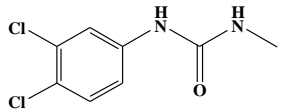
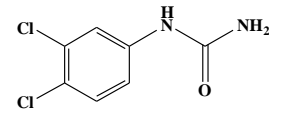
281 **Figure 3** Effect of the cytochrome P450 inhibitor 1-aminobenzotriazole on the degradation of
282 diuron by *T. versicolor*. C represents the residual concentration of diuron in the sample (mg L^{-1}),
283 and C_0 corresponds to the initial concentration of diuron in the sample (mg L^{-1}); *Filled squares*,
284 inhibitor-free; *empty circles*, inhibitor. Average values of three replicates with the corresponding
285 standard deviation are shown.

286 3.3. TPs generated during degradation of diuron by *T. versicolor*

287 Main TPs generated during the degradation of diuron by *T. versicolor* and detected using LC-
288 HRMS are shown in Table 2. In total five ions were identified as TPs; however, logical tentative
289 structures could be only proposed for three of them with an identification confidence level of 3 (CL3)
290 according to Schymanski's scale (Schymanski et al., 2014). The remaining two TPs were appointed
291 as "unequivocal molecular formulae" (identification confidence level of 4), as no sufficient evidence
292 existed to propose possible structures. The CL3 TPs were TP248 3-(3,4-dichlorophenyl)-1-
293 hydroxymethyl-1-methylurea (DCPHMU), TP218 3-(3,4-dichlorophenyl)-1-methylurea (DCPMU),
294 and TP204 3,4-dichlorophenylurea (DCPU). TP218 (DCPMU) and TP204 (DCPU) have been
295 previously reported as aerobic degradation by-products of diuron regardless of the organism
296 (bacteria or fungi) used for its degradation. They are formed after successive N-demethylations
297 reactions of diuron (Badawi et al., 2009; Coelho-Moreira et al., 2013, 2018; Ellegaard-Jensen et al.,
298 2014; Sørensen et al., 2008). Demethylation of diuron may occur intracellularly, as diuron and these
299 demethylated metabolites were found to be present in mycelial extracts of *G. lucidum* (Coelho-
300 Moreira et al., 2018). This is also in agreement with the results obtained in the laccase experiments
301 conducted in this study. All identified TPs remained in solution after 7 days of treatment; however,
302 TP204 (DCPU), TP137 and TP195 were the ones that presented an increasing trend by the end of
303 the experiment. Thus, TP248 (DCPHMU) and TP218 (DCPMU) can be considered as intermediate
304 byproducts that further degrade in contact with the fungus (Figure S1 in SI). TP248 is believed to
305 be formed after carbon hydroxylation at the tertiary amine moiety. This reaction may be mediated
306 by the cytochrome P450 system, according to the enzymatic exploration results and to a previous
307 study on the detoxification of chlortoluron by the grass weed *A. myosuroides* (Hall et al., 1995).

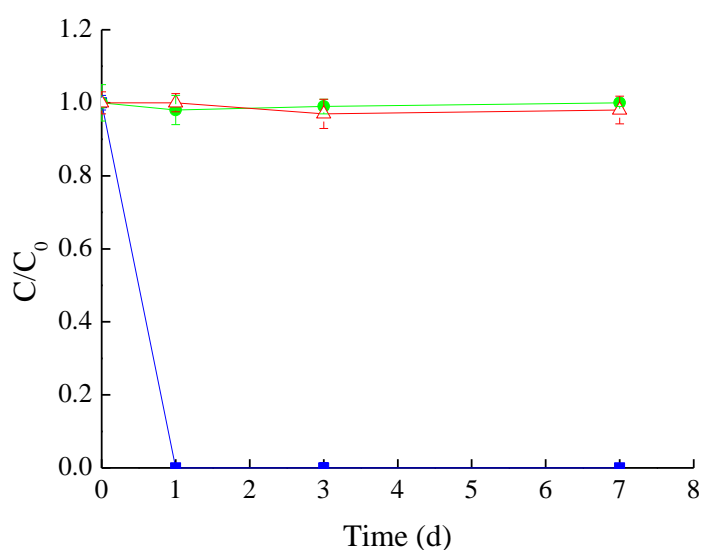
308 This is the first report of the formation of TP248 during microbial degradation of diuron.

309 **Table 2** Transformation products formed during diuron degradation by *T. versicolor*

Number	t_R (min)	HESI mode	Full Scan			MS/MS				Suspect identity (Confidence level)	Chemical structure	
			m/z	Formula	RDB	Δm (ppm)	m/z	Formula	RDB			Δ (ppm)
TP248	6.7	-	247.0030	C ₉ H ₉ O ₂ N ₂ Cl ₂	5.5	-2.1	159.9708	C ₆ H ₄ NCl ₂	4.5	-4.6	DCPHMU (CL3)	
TP218	8.6	+	219.0093	C ₈ H ₉ Cl ₂ ON ₂	4.5	3.3	161.9876	C ₆ H ₆ Cl ₂ N	3.5	3.8	DCPMU (CL3)	
TP204	8.5	+	204.9937	C ₇ H ₆ Cl ₂ N ₂ O	4.5	3.5	161.9877	C ₆ H ₆ Cl ₂ N	3.5	3.4	DCPU (CL3)	
							159.9728	C ₆ H ₄ Cl ₂ N	4.5	8.2		
							92.0503	C ₆ H ₆ N	4.5	8.5		
TP137	2.9	+	138.0556	C ₇ H ₈ O ₂ N	4.5	4.4	110.0608	C ₆ H ₈ ON	3.5	7.1	n/a (CL4)	
TP195	4.3	+	196.0612	C ₉ H ₁₀ O ₄ N	5.5	4.0	178.0508	C ₉ H ₈ O ₃ N	6.5	3.6	n/a (CL4)	
							150.0556	C ₈ H ₈ O ₂ N	5.5	4.5		

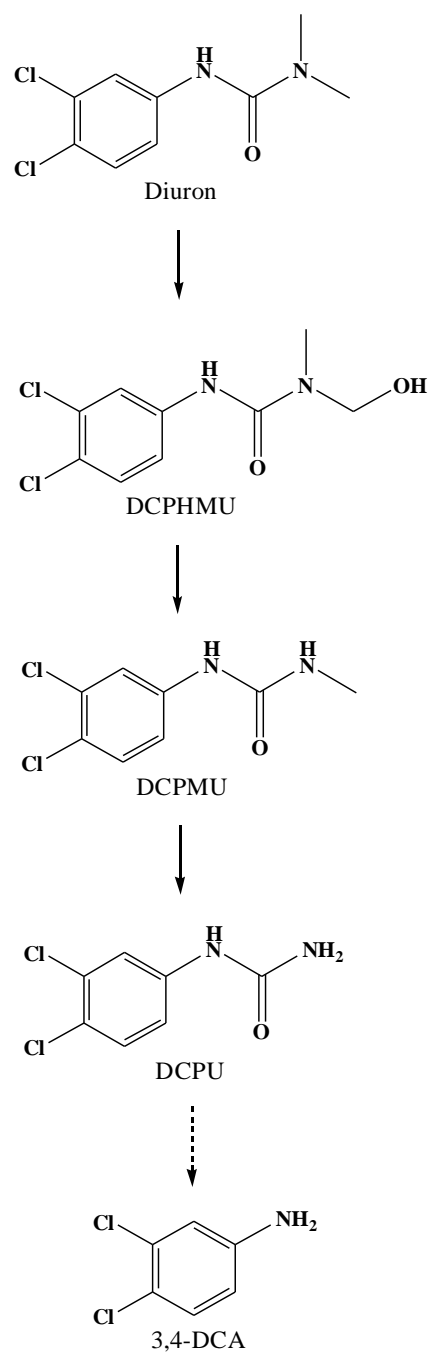
310 t_R : chromatographic retention time, HESI, heated-electrospray ionization; Δm , mass measurement error; RDB, ring and double-bound equivalents

311 3,4-DCA has been widely reported to be a diuron TP that could be generated after the amide bond
312 hydrolysis of DCPU; however, it was not detected in the experimental culture media in this study.
313 Since 3,4-DCA is much more toxic than diuron, the ability of *T. versicolor* to remove this TP was
314 also evaluated. A degradation experiment using 3,4-DCA as substrate was conducted. *T. versicolor*
315 showed an exceptional ability to degrade 3,4-DCA Initial 3,4-DCA concentrations (10 mg L^{-1}) were
316 degraded in less than 24 h (Figure 4). This may explain why 3,4-DCA was not identified as a diuron
317 TP in this study. The biodegradation of 3,4-DCA under aerobic conditions has been extensively
318 described, and it could be reduced to a dechlorination step followed by ring-cleavage (Giacomazzi
319 and Cochet, 2004; Tasca and Fletcher, 2018).



320
321 **Figure 4** Time-course degradation of 3,4-DCA by *T. versicolor*. C represents the residual
322 concentration of 3,4-DCA in the sample (mg L^{-1}), and C_0 corresponds to the initial concentration
323 of 3,4-DCA in the sample (mg L^{-1}); Blue lines with filled squares, experimental; red lines with
324 empty triangles, killed control; green lines with filled circles, abiotic. Average values of three
325 replicates with the corresponding standard deviation are shown.
326

327 Based on our results and previous findings, a pathway of diuron degradation by *T. versicolor* is
328 proposed in Figure 5; however, further investigation is still needed to understand the entire
329 metabolic pathway.



330

331 **Figure 5** Proposed pathway of diuron degradation by *T. versicolor*. *Full lines*, the reactions
 332 observed in this study; *dashed lines*, the reaction described in the literature

333

334 3.4. Influence of operational variables on diuron removal using TBR under non-sterile condition

335 TBR performance is difficult to describe using a mathematical model due to the various physical
 336 and biological processes involved in it. On one side, the contribution of the wood is not limited to
 337 the immobilization of the biomass. It also plays an important role in pollutant removal due to

338 adsorption, which occurs mainly in the early stages of a continuous treatment process. On the other
339 side, wood is a nutrient source that promotes fungal growth. The water is distributed from the bottom
340 to the top of the TBR and flows through a bed with a remarkably high porosity (60%), which is
341 mainly occupied by air. Thus, the removal yield will depend mainly on the contact time between the
342 immobilized biomass and the liquid phase. The biomass is directly related to the mass of the wood,
343 referred to as the working volume of the bioreactor (V_R) (Fig. 1). Since the working volume (V_R)
344 and the HRT were fixed, the factors amenable to modification were narrowed down to the
345 recirculation flow rate (F_r), the influent flow rate (F_{in}), and the water volume in the reservoir tank
346 (V_r). The number of times that the water is recirculated through the bioreactor is designated as RR
347 (F_r/F_{in}). The HRT, defined as the ratio between the volume of water in the system (i.e., the volume
348 of water in the reservoir tank (V_r)) and the F_{in} , was fixed to 3 days according to previous experiences
349 (Torán et al., 2017). The ratio between F_{in} and V_R stands for the pollutant load to the system.
350 Therefore, the factors RR (X_1) and F_{in}/V_R (X_2) were selected for studying each effect, as well as
351 their interaction on the removal of diuron. According to the factorial experimental design with 3
352 levels for each of these two factors, 12 trials were performed using tap water fortified with diuron,
353 and each experimental result along with model predicted values are given in Table 3.

354

355 **Table 3** Central Composite Design matrix showing actual and predicted values for diuron removal

Run	Factors in coded value		Response (Diuron removal, %)	
	X_1	X_2	Actual	Predicted
1	0	-1	74.4	74.1
2	1	-1	67.3	66.9
3	1	0	44.7	44.1
4	0	0	56.7	56.1
5	-1	0	64.6	68.2
6	-1	-1	83.0	81.2

7	1	1	26.5	21.3
8	-1	1	62.6	55.2
9	0	0	29.5	38.2
10	-1	-1	84.0	81.2
11	-1	-1	82.0	81.2
12	-1	-1	78.0	81.2

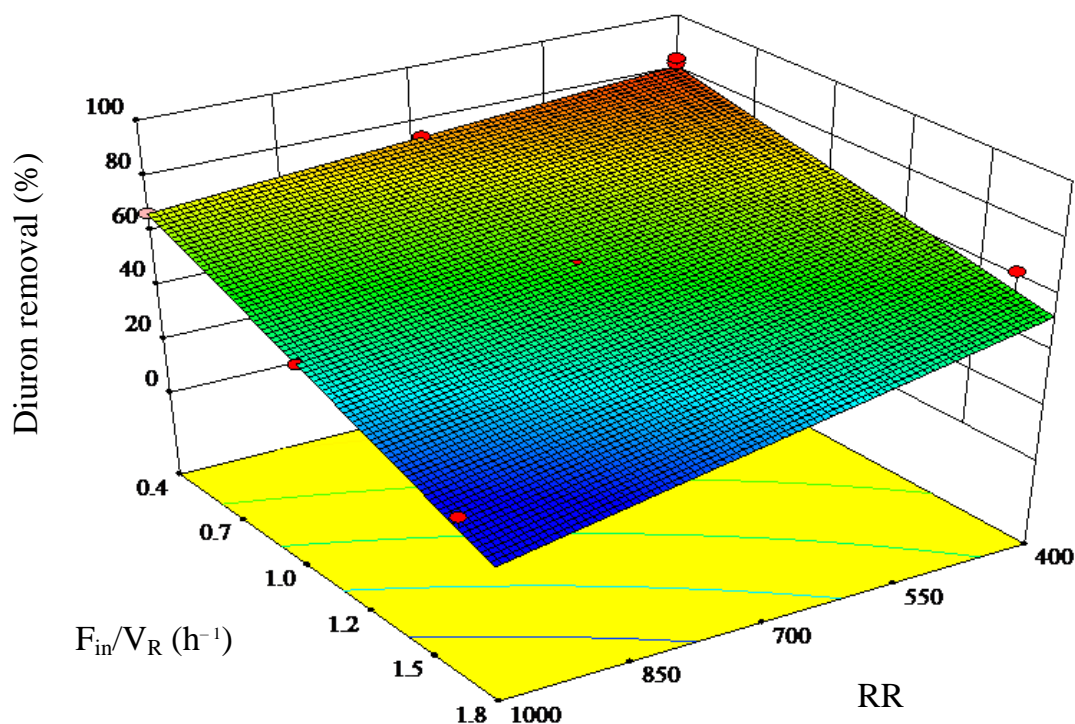
356

357 In each trial, the packing material was renovated to avoid fungus aging and adverse effect of
 358 saturated wood on adsorption. The response of each run was the mean removal value obtained
 359 during the steady state, which was achieved from day 9 to day 18 of continuous operation. Based
 360 on the fitness of the data obtained, the following linear regression model for diuron removal in the
 361 TBR system is proposed:

$$Y = 56.61 - 11.98X_1 - 17.72X_2 - 5.05X_1X_2 \quad (1)$$

362 To further verify the goodness of the proposed model for diuron removal, analysis of variance
 363 (ANOVA) was applied (Table S3 in SI). The results obtained indicate that the proposed model is
 364 significant with a confidence level of 95% ($F = 58.54, p < 0.0001$), which also addressed its stability.
 365 The adjusted R^2 was 0.9401, indicating that 94 % of the data variance could be explained by the
 366 studied factors (with a level of confidence of 95%). The two factors and the interaction between
 367 them were also significant to predict diuron removal ($p < 0.05$) on which the predictor F_{in}/V_R
 368 demonstrate highest effect. The lack of fit was non-significant, which evidences the good correlation
 369 between the experimental factors or predictors and the response variable. Besides, Table 3 shows
 370 the agreement between the experimental data and those predicted by the model. Figure 6 illustrates
 371 that the decrease in RR and F_{in}/V_R enhanced the removal of diuron. Therefore, it is clear to infer
 372 here the improvement of yield that can be obtained by setting those two factors at the lowest possible
 373 levels, having in mind the following condition as V_R is constant.

$$\frac{\Delta F_r}{F_r} < \frac{\Delta F_{in}}{F_{in}} \quad (2)$$



374

375 **Figure 6** Response surface showing the effects of RR and F_{in}/V_R on diuron removal

376

377 The results evidenced, as expected, that the lower the volumetric load (F_{in}/V_R) the higher the

378 pollutant removal, but also that lower recirculating rates entail better removal yields. The RR is

379 related to the times that the water is passed through the bioreactor. In this regard, according to our

380 results, and contrary to expected, low RR values result in better performance than high RR values.

381 This could be explained by the fact that the highest contact time between the immobilized fungus

382 and the pollutant may contribute considerably to increase the removal efficiency, which is also

383 consistent with the fact that the cytochrome P450 system was the one found to be involved in diuron

384 degradation instead of extracellular enzymes. High RR requires high recirculating flow rates

385 promoting a coalescing effect between water drops, which increases the crossing velocity through

386 the column and consequently results in a reduction of the contact time with the fungus. However, a

387 lower value of diuron removal (72% vs 81.2%) was obtained in an additional experiment using RR

388 of 200 and optimal F_{in}/V_R . This result indicates that better removal could be achieved by enlarging
389 the experimental domain to the corner where the optimum is. In summary, to design an effective
390 TBR is important to ensure a high contact time between the water and the fungus. This will depend
391 on the operational parameters that further influence the water crossing velocity through the
392 bioreactor.

393

394 **4. Conclusions**

395 Of the four fungi species investigated, *T. versicolor* was found to be the one that most efficiently
396 degraded both diuron and its main byproduct 3,4-DCA. The cytochrome P450 enzymatic system
397 was found to be the one catalyzing diuron removal. Up to five TPs were formed during the process,
398 and structures could be tentatively proposed for three of them. One intermediate TP, namely
399 DCPHMU, was detected for the first time, providing a better understanding of the occurring
400 demethylation process. The effect of operational variables on diuron removal from water using a
401 trickle-bed reactor was also evaluated. The contact time between the immobilized fungus and the
402 water played an important role in diuron removal. This represents a pioneering step forward to
403 overcome key barriers to upscale this type of bioreactor and apply this technology to the
404 bioremediation for real diuron-contaminated waters since the TBR tested in this study was operated
405 under non-sterile conditions.

406

407 **Acknowledgment**

408 This work has been supported by the Spanish Ministry of Economy and Competitiveness State
409 Research Agency (CTM2016-75587-C2-1-R and CTM2016-75587-C2-2-R) and co-financed by the

410 European Union through the European Regional Development Fund (ERDF) and the Horizon 2020
411 research and innovation WATERPROTECT project (727450). This work was partly supported by
412 the Generalitat de Catalunya (Consolidate Research Group 2017-SGR-14) and the Ministry of
413 Science and Innovation (Project CEX2018-000794-S). The Department of Chemical, Biological and
414 Environmental Engineering of the Universitat Autònoma de Barcelona is a member of the Xarxa de
415 Referència en Biotecnologia de la Generalitat de Catalunya. K. Hu acknowledges the financial
416 support from the Chinese Scholarship Council.

417

418 **Conflict of interest**

419 We declare that no conflict of interest exists in the submission of this manuscript.

420

421 **References**

- 422 Azubuike, C.C., Chikere, C.B., Okpokwasili, G.C., 2016. Bioremediation techniques-classification
423 based on site of application: principles, advantages, limitations and prospects. World J. Microb.
424 Biot. 32, 180. <https://doi.org/10.1007/s11274-016-2137-x>.
- 425 Badawi N., Rønhede, S., Olsson, S., Kragelund, B.B., Johnsen, A.H., Jacobsen, O.S, Aamand, J.,
426 2009. Metabolites of the phenylurea herbicides chlorotoluron, diuron, isoproturon and linuron
427 produced by the soil fungus *Mortierella* sp. Environ. Pollut. 157, 2806-2812.
428 <https://doi.org/10.1016/j.envpol.2009.04.019>.
- 429 Bhattacharya, S., Das, A., Prashanthi, K., Palaniswamy, M., Angayarkanni, J., 2014.
430 Mycoremediation of Benzo[a]pyrene by *Pleurotus ostreatus* in the presence of heavy metals
431 and mediators. 3 Biotech. 4, 205-211. <https://doi.org/10.1007/s13205-013-0148-y>.

432 Bilal, M., Iqbal, H.M., Barceló, D., 2019. Persistence of pesticides-based contaminants in the
433 environment and their effective degradation using laccase-assisted biocatalytic systems. *Sci.*
434 *Total Environ.* 695, 133896. <https://doi.org/10.1016/j.scitotenv.2019.133896>.

435 Blánquez, P., Casas, N., Font, X., Gabarrell, X., Sarrà, M., Caminal, G., Vicent, T., 2004.
436 Mechanism of textile metal dye biotransformation by *Trametes versicolor*. *Water Res.* 38,
437 2166-2172. <https://doi.org/10.1016/j.watres.2004.01.019>.

438 Coelho-Moreira, J., Bracht, A., de Souza, A., Oliveira, R., de Sá-Nakanishi, A., de Souza C., Peralta,
439 R., 2013. Degradation of diuron by *Phanerochaete chrysosporium*: role of ligninolytic
440 enzymes and cytochrome P450. *BioMed Res. Int.* 2013. <https://doi.org/10.1155/2013/251354>.

441 Coelho-Moreira, J., Brugnari, T., Sá-Nakanishi, A., Castoldi, R., de Souza, C., Bracht, A., Peralta,
442 R., 2018. Evaluation of diuron tolerance and biotransformation by the white-rot fungus
443 *Ganoderma lucidum*. *Fungal Biol-UK* 122: 471-478.
444 <https://doi.org/10.1016/j.funbio.2017.10.008>.

445 da Luz, J., Paes, S., Nunes, M., da Silva M., Kasuya, M., 2013. Degradation of oxo-biodegradable
446 plastic by *Pleurotus ostreatus*. *PLoS ONE* 8, e69386.
447 <https://doi.org/10.1371/journal.pone.0069386>.

448 Directive 2013. Directive 2013/39/EU of the European Parliament and of the Council of 12 August
449 2013 amending Directives 2000/60/EC and 2008/105/EC as regards priority substances in the
450 field of water policy. *Off J. Eur. Union* 226, 1-17.

451 Ellegaard-Jensen, L., Aamand, J., Kragelund, B.B., Johnsen, A.H., Rosendahl, S., 2013. Strains of
452 the soil fungus *Mortierella* show different degradation potentials for the phenylurea herbicide
453 diuron. *Biodegradation* 24, 765-774. <https://doi.org/10.1007/s10532-013-9624-7>.

454 Ellegaard-Jensen, L., Knudsen, B.E., Johansen, A., Albers, C.N., Aamand, J., Rosendahl, S., 2014.
455 Fungal-bacterial consortia increase diuron degradation in water-unsaturated systems. *Sci. Total*
456 *Environ.* 466, 699-705. <https://doi.org/10.1016/j.scitotenv.2013.07.095>.

457 Giacomazzi, S., Cochet, N., 2004. Environmental impact of diuron transformation: a review.
458 *Chemosphere* 56, 1021-1032. <https://doi.org/10.1016/j.chemosphere.2004.04.061>.

459 Glazunova, O.A., Trushkin, N.A., Moiseenko, K.V., Filimonov, I.S., Fedorova, T.V., 2018. Catalytic
460 efficiency of basidiomycete laccases: redox potential versus substrate-binding pocket structure.
461 *Catalysts* 8, 152. <https://doi.org/10.3390/catal8040152>.

462 Hall, L., Moss, S., Powles, S., 1995. Mechanism of resistance to chlorotoluron in two biotypes of
463 the grass weed *Alopecurus myosuroides*. *Pestic. Biochem. Phys.* 53, 180-192.
464 <https://doi.org/10.1006/pest.1995.1066>.

465 Huovinen, M., Loikkanen, J., Naarala, J., Vähäkangas, K., 2015. Toxicity of diuron in human cancer
466 cells. *Toxicol. in Vitro* 29, 1577-1586. <https://doi.org/10.1016/j.tiv.2015.06.013>.

467 Kaonga, C.C., Takeda, K., Sakugawa, H., 2015. Diuron, Irgarol 1051 and Fenitrothion
468 contamination for a river passing through an agricultural and urban area in Higashi Hiroshima
469 City, Japan. *Sci. Total Environ.* 518, 450-458. <https://doi.org/10.1016/j.scitotenv.2015.03.022>

470 Kirk, T.K., Schultz, E., Connors, W., Lorenz, L., Zeikus, J., 1978. Influence of culture parameters
471 on lignin metabolism by *Phanerochaete chrysosporium*. *Arch. Microbiol.* 117, 277-285.
472 <https://doi.org/10.1007/BF00738547>.

473 López-Ramón, M.V., Rivera-Utrilla, J., Sánchez-Polo, M., Polo A.M.S., Mota, A.J., Orellana-
474 García, F., Álvarez, M.A., 2019. Photocatalytic oxidation of diuron using nickel organic
475 xerogel under simulated solar irradiation. *Sci. Total Environ.* 650, 1207-1215.

476 <https://doi.org/10.1016/j.scitotenv.2018.09.113>.

477 Langeron, J., Sayen, S., Couderchet, M., Guillon, E., 2014. Leaching potential of phenylurea
478 herbicides in a calcareous soil: comparison of column elution and batch studies. *Environ. Sci.*
479 *Pollut. R.* 21, 4906-4913. <https://doi.org/10.1007/s11356-012-1244-y>.

480 Liu, J., 2014. Diuron, , in: Richardson, R.J. (3rd), *Encyclopedia of toxicology*. Amsterdam: Elsevier,
481 pp. 215-216.

482 Liu, J., Morales-Narváez, E., Vicent, T., Merkoçi A, Zhong, G., 2018. Microorganism-decorated
483 nanocellulose for efficient diuron removal. *Chem. Eng. J.* 354, 1083-1091.
484 <https://doi.org/10.1016/j.cej.2018.08.035>.

485 Llorca, M., Castellet-Rovira, F., Farré, M.J., Jaén-Gil, A., Martínez-Alonso, M., Rodríguez-Mozaz,
486 S., Sarrà, M., Barceló, D., 2019. Fungal biodegradation of the N-nitrosodimethylamine
487 precursors venlafaxine and O-desmethylvenlafaxine in water. *Environ. Pollut.* 246, 346-356.
488 <https://doi.org/10.1016/j.envpol.2018.12.008>.

489 Lucas, D., Castellet-Rovira, F., Villagrasa, M., Badia-Fabregat, M., Barceló, D., Vicent, T., Caminal,
490 G., Sarrà, M, Rodríguez-Mozaz, S., 2018. The role of sorption processes in the removal of
491 pharmaceuticals by fungal treatment of wastewater. *Sci. Total Environ.* 610, 1147-1153.
492 <https://doi.org/10.1016/j.scitotenv.2017.08.118>.

493 Luo, Y., Guo, W., Ngo, H.H., Nghiem, L.D., Hai, F.I., Zhang, J., Liang, S., Wang, X., 2014. A review
494 on the occurrence of micropollutants in the aquatic environment and their fate and removal
495 during wastewater treatment. *Sci. Total Environ.* 473, 619-641.
496 <https://doi.org/10.1016/j.scitotenv.2013.12.065>.

497 Mansano, A.S., Moreira, R.A., Dornfeld, H.C., Diniz, L.G., Vieira, E.M., Daam, M.A., Rocha, O.,

498 Selegim, M.H., 2018. Acute and chronic toxicity of diuron and carbofuran to the neotropical
499 cladoceran *Ceriodaphnia silvestrii*. Environ. Sci. Pollut. R. 25, 13335-13346.
500 <https://doi.org/10.1007/s11356-016-8274-9>

501 Marco-Urrea, E., Pérez-Trujillo, M., Vicent, T., Caminal, G., 2009. Ability of white-rot fungi to
502 remove selected pharmaceuticals and identification of degradation products of ibuprofen by
503 *Trametes versicolor*. Chemosphere 74, 765-772.
504 <https://doi.org/10.1016/j.chemosphere.2008.10.040>.

505 Mir-Tutusaus, J.A., Baccar, R., Caminal, G., Sarrà, M., 2018. Can white-rot fungi be a real
506 wastewater treatment alternative for organic micropollutants removal? A review. Water res.
507 138, 137-151. <https://doi.org/10.1016/j.watres.2018.02.056>.

508 Palli, L., Castellet-Rovira, F., Pérez-Trujillo, M., Caniani, D., Sarrà, M., Gori, R., 2017. Preliminary
509 evaluation of *Pleurotus ostreatus* for the removal of selected pharmaceuticals from hospital
510 wastewater. Biotechnol. Progr. 33, 1529-1537. <https://doi.org/10.1002/btpr.2520>.

511 Palli, L., Gullotto, A., Tilli, S., Gori, R., Lubello, C., Scozzafava, A., 2014. Effect of carbon source
512 on the degradation of 2-naphthalenesulfonic acid polymers mixture by *Pleurotus ostreatus* in
513 petrochemical wastewater. Process Biochem. 49, 2272-2278.
514 <https://doi.org/10.1016/j.procbio.2014.08.015>.

515 Purnomo AS, Mori T, Kamei I, Nishii T, Kondo R. Application of mushroom waste medium from
516 *Pleurotus ostreatus* for bioremediation of DDT-contaminated soil. International
517 Biodeterioration & Biodegradation 2010; 64: 397-402.

518 Purnomo, A.S., Nawfa, R., Martak, F., Shimizu, K., Kamei, I., 2017. Biodegradation of aldrin and
519 dieldrin by the white-rot fungus *Pleurotus ostreatus*. Curr. Microbiol. 74, 320-324.

520 <https://doi.org/10.1007/s00284-016-1184-8>.

521 Rippy M.A., Deletic, A., Black, J., Aryal, R., Lampard, J.L., Tang, J.Y.M., McCarthy, D., Kolotelo,
522 P., Sidhu, J., Gernjak, W., 2017. Pesticide occurrence and spatio-temporal variability in urban
523 run-off across Australia. *Water Res.* 115, 245-255.
524 <https://doi.org/10.1016/j.watres.2017.03.010>.

525 Sørensen, S.R., Albers, C.N., Aamand, J., 2008. Rapid mineralization of the phenylurea herbicide
526 diuron by *Variovorax* sp. strain SRS16 in pure culture and within a two-member consortium.
527 *Appl. Environ. Microbiol.* 74, 2332-2340. <https://doi.org/10.1128/AEM.02687-07>.

528 Santos, E.A., Correia, N.M., Silva, J.R.M., Velini, E.D., Passos, A.B.R.J, Durigan, J.C., 2015.
529 Herbicide detection in groundwater in Córrego Rico-SP watershed. *Planta Daninha* 33, 147-
530 155. <https://doi.org/10.1590/S0100-83582015000100017>.

531 Santos, L.H., Freixa, A., Insa, S., Acuña, V., Sanchís, J., Farré, M., Sabater, S., Barceló, D.,
532 Rodríguez-Mozaz, S., 2019. Impact of fullerenes in the bioaccumulation and biotransformation
533 of venlafaxine, diuron and triclosan in river biofilms. *Environ. Res.* 169: 377-386.
534 <https://doi.org/10.1016/j.envres.2018.11.036>.

535 Schymanski, E.L., Jeon, J., Gulde, R., Fenner, K., Ruff, M., Singer, H.P., Hollender, J., 2014.
536 Identifying small molecules via high resolution mass spectrometry: communicating confidence.
537 *Environ. Sci. Technol.* 48, 2097-2098. <https://doi.org/10.1021/es5002105>.

538 Sharma, P., Chopra, A., Cameotra, S.S., Suri, C.R., 2010. Efficient biotransformation of herbicide
539 diuron by bacterial strain *Micrococcus* sp. PS-1. *Biodegradation* 21, 979-987.
540 <https://doi.org/10.1007/s10532-010-9357-9>.

541 Singh, A.P., Singh, T., 2014. Biotechnological applications of wood-rotting fungi: A review.

542 Biomass and Bioenerg. 62, 198-206. <https://doi.org/10.1016/j.biombioe.2013.12.013>.

543 Tasca, A.L., Fletcher, A., 2018. State of the art of the environmental behaviour and removal
544 techniques of the endocrine disruptor 3, 4-dichloroaniline. J. Environ. Sci. Heal. A 53, 260-
545 270. <https://doi.org/10.1080/10934529.2017.1394701>.

546 Torán, J., Blánquez, P., Caminal, G., 2017. Comparison between several reactors with *Trametes*
547 *versicolor* immobilized on lignocellulosic support for the continuous treatments of hospital
548 wastewater. Bioresource Technol. 43, 966-974. <https://doi.org/10.1016/j.biortech.2017.07.055>.

549 Villaverde, J., Rubio-Bellido, M., Merchán, F., Morillo, E., 2017. Bioremediation of diuron
550 contaminated soils by a novel degrading microbial consortium. J. Environ. Manage. 188, 379-
551 386. <https://doi.org/10.1016/j.jenvman.2016.12.020>.

552 Wariishi, H., Valli, K., Gold, M.H., 1992. Manganese (II) oxidation by manganese peroxidase from
553 the basidiomycete *Phanerochaete chrysosporium*. Kinetic mechanism and role of chelators. J.
554 Biol. Chem. 267, 23688-23695.

Supplementary information

Fungal bioremediation of diuron-contaminated waters: evaluation of its degradation and the effect of amendable factors on its removal in a trickle-bed reactor under non-sterile conditions

Kaidi Hu¹, Josefina Torán¹, Ester López-García², Maria Vittoria Barbieri², Cristina Postigo², Miren López de Alda², Gloria Caminal³, Montserrat Sarrà^{1*}, Paqui Blánquez¹

¹Departament d'Enginyeria Química, Biològica i Ambiental, Escola d'Enginyeria, Universitat Autònoma de Barcelona, 08193 Bellaterra, Barcelona, Spain

²Water, Environmental and Food Chemistry Unit (ENFOCHEM), Department of Environmental Chemistry, Institute of Environmental Assessment and Water Research (IDAEA), Spanish Council for Scientific Research (CSIC), Jordi Girona 18-26, 08034 Barcelona, Spain

³Institut de Química Avançada de Catalunya (IQAC), CSIC. Jordi Girona 18-26, 08034 Barcelona, Spain

***Corresponding author:** Departament d'Enginyeria Química, Biològica i Ambiental, Escola d'Enginyeria, Universitat Autònoma de Barcelona, 08193 Bellaterra, Barcelona, Spain. Tel: + 34-34935812789; E-mail: montserrat.sarra@uab.cat

Table S1 Time-course of glucose concentrations in the experimental culture media (g L⁻¹)

Fungus	Incubation time (d)			
	0	1	3	7
<i>T. versicolor</i>	7.00 ± 0.13	5.35 ± 0.16	1.83 ± 0.40	< 0.01
<i>G. luteofolius</i>	6.63 ± 0.10	4.77 ± 0.02	0.54 ± 0.29	< 0.01
<i>S. rugosoannulata</i>	7.02 ± 0.13	4.34 ± 0.02	< 0.01	ND
<i>P. ostreatus</i>	7.01 ± 0.12	6.21 ± 0.09	5.67 ± 0.05	4.85 ± 0.10

Note: Each value of glucose concentration represents the mean of triplicate measurements ± SD.

ND: no detected

Table S2 Effect of laccase on diuron degradation in the presence and absence of mediators

Time (h)	Diuron (mg L^{-1})				
	Abiotic control	Laccase	VA	ABTS	HOBt
0	10.01 ± 0.41	9.69 ± 0.91	9.02 ± 0.31	9.58 ± 0.72	9.41 ± 0.29
8	9.83 ± 0.38	9.74 ± 0.59	8.96 ± 0.47	10.35 ± 0.21	9.25 ± 0.71
24	9.45 ± 0.75	9.40 ± 0.60	9.69 ± 0.49	9.66 ± 0.35	10.60 ± 0.83
72	9.32 ± 1.10	9.01 ± 0.89	9.54 ± 1.10	10.74 ± 0.16	9.13 ± 1.47

Note: Each value of laccase concentration represents the mean of triplicate measurements \pm SD. VA, violuric acid monohydrate; ABTS, 2,2'-azino-bis (3-ethylbenzothiazoline-6-sulphonic acid) diammonium salt; HOBt, hydrated 1-hydroxybenzotriazole

Table S3 Analysis of variance of the linear regression model proposed

Source	Sum of squares	Degrees of freedom	Mean square	F	<i>p</i>
Model	4, 214.66	3	1, 404.89	58.54	< 0.0001*
X ₁	1, 028.52	1	1, 028.52	42.86	0.0002*
X ₂	2, 248.02	1	2, 248.02	93.68	< 0.0001*
X ₁ X ₂	134.73	1	134.73	5.61	0.0454*
Residual	191.98	8	24.00		
Lack of fit	171.23	5	34.25	4.95	0.1091
Pure error	20.75	3	6.92		
Total	4, 406.64	11			

*Significant ($p < 0.05$)

$R^2 = 0.9564$

$R^2_{\text{adj}} = 0.9401$

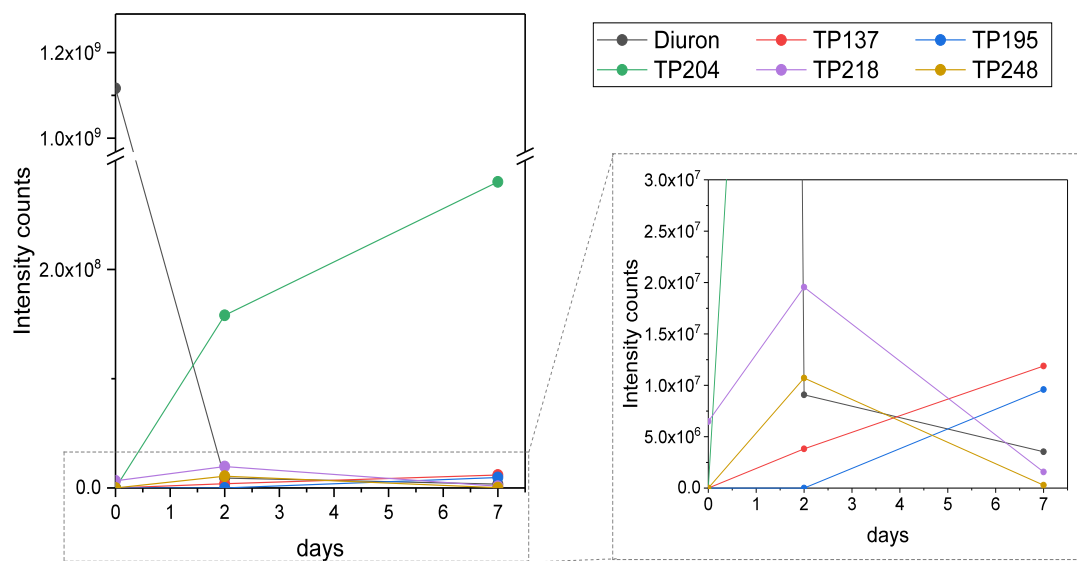


Figure S1. Evolution of the TPs identified during *T. versicolor*-mediated degradation of diuron